Cellular/Molecular

MT3-MMP Promotes Excitatory Synapse Formation by Promoting Nogo-66 Receptor Ectodomain Shedding

Ricardo L. Sanz,[1] Gino B. Ferraro,[1] Johannes Kacervosky,[2] Charleen Salesse,[3] Elizabeth Gowing,[1] Luyang Hua,[1] Isabel Rambaldi,[1] Francois Beaubien,[1] Kenn Holmbeck,[4] J.F. Cloutier,[1] Martin Lévesque,[3] Keith Murai,[2] and Alyson E. Fournier[1]

[1]Department of Neurology and Neurosurgery, Montréal Neurological Institute, Rue University, Montréal, Québec H3A 2B4, Canada, [2]Centre for Research in Neuroscience, Department of Neurology and Neurosurgery, The Research Institute of the McGill University Health Centre, Montreal General Hospital, Montréal, Québec H3G 1A4, Canada, [3]Department of Psychiatry and Neuroscience, Université Laval, CERVO Brain Research Centre, Québec, Québec G1V 0A6, Canada, and [4]Craniofacial and Skeletal Diseases Branch, NIDCR, National Institutes of Health (NIH), Bethesda, Maryland 20892-4380

Cell-surface molecules are dynamically regulated at the synapse to assemble and disassemble adhesive contacts that are important for synaptogenesis and for tuning synaptic transmission. Metalloproteinases dynamically regulate cellular behaviors through the processing of cell surface molecules. In the present study, we evaluated the role of membrane-type metalloproteinases (MT-MMPs) in excitatory synaptogenesis. We find that MT3-MMP and MT5-MMP are broadly expressed in the mouse cerebral cortex and that MT3-MMP loss-of-function interferes with excitatory synapse development in dissociated cortical neurons and in *vivo*. We identify Nogo-66 receptor (NgR1) as an MT3-MMP substrate that is required for MT3-MMP-dependent synapse formation. Introduction of the shed ectodomain of NgR1 is sufficient to accelerate excitatory synapse formation in dissociated cortical neurons and in *vivo*. Together, our findings support a role for MT3-MMP-dependent shedding of NgR1 in regulating excitatory synapse development.

Key words: **metalloproteinase; Nogo receptor; synaptogenesis**

Significance Statement

In this study, we identify MT3-MMP, a membrane-bound zinc protease, to be necessary for the development of excitatory synapses in cortical neurons. We identify Nogo-66 receptors (NgR1) as a downstream target of MT3-MMP proteolytic activity. Furthermore, processing of surface NgR1 by MT3-MMP generates a soluble ectodomain fragment that accelerates the formation of excitatory synapses. We propose that MT3-MMP activity and NgR1 shedding could stimulate circuitry remodeling in the adult brain and enhance functional connectivity after brain injury.

Introduction

The functionality of the mammalian CNS depends on the formation of a precise network of synaptic contacts that actively change their strength, morphology and density throughout life (Florence et al., 1998; Fu and Zuo, 2011). Extracellular matrix and synaptic components are subject to proteolysis, a mechanism that alters protein function and allows circuit remodelling (Dityatev and Schachner, 2003; Gundelfinger et al., 2010; Sanz et al., 2017). A better understanding of the molecular and cellular mechanisms that dictate how synapse formation is regulated could lead to therapies to promote functional synaptic recovery after injury, treat neurological disorders, and increase cognitive function.

In the nervous system, members of the metalloproteinase subfamily, Matrix metalloproteinases and adamalysins, mediate proteolytic processing of membrane-anchored precursors and the subsequent release of biologically active, or dominant-negative fragments. Membrane-type metalloproteinases (MT-MMPs) are members of the zinc endopeptidase subfamily of matrix metalloproteinases (MMPs). They are transmembrane proteases that release surface proteins through a mechanism termed ectodomain shedding. Metalloproteinase activity is controlled through removal of a repressive propeptide domain and the expression of endogenous inhibitors called tissue inhibitor of metalloproteinases (TIMPs). At the subcellular level, MT-MMPs are present in

Received April 4, 2017; revised Oct. 23, 2017; accepted Nov. 20, 2017.

Author contributions: R.L.S., G.B.F., J.K., E.G., L.H., I.R., F.B., J.F.C., M.L., K.M., and A.E.F. designed research; R.L.S., G.B.F., J.K., C.S., E.G., L.H., I.R., F.B., and K.H. performed research; R.L.S., G.B.F., J.K., C.S., E.G., I.R., F.B., K.H., J.F.C., M.L., K.M., and A.E.F. analyzed data; R.L.S., G.B.F., J.F.C., M.L., K.M., and A.E.F. wrote the paper.

This work was supported by Grants from the Canadian Institutes of Health Research and Natural Sciences and Engineering Research Council of Canada (A.E.F.), the McGill Program in Neuroengineering, and a Jeanne Timmins Costello Studentship (R.S.).

The authors declare no competing financial interests.

Correspondence should be addressed to Dr. Alyson Fournier, Montréal Neurological Institute, BT-109, 3801, Rue University, Montréal, QC H3A 2B4, Canada. E-mail: alyson.fournier@mcgill.ca.

DOI:10.1523/JNEUROSCI.0962-17.2017

 0270-6474/18/380518-12$15.00/0

dendritic spines and proteolytic activity is largely absent from GABAergic synapses, suggesting a potential role in excitatory synaptogenesis. Ectodomain shedding targets inhibitory or permissive membrane-anchored substrates that alter synapse rearrangements (Lim et al., 2012; Peixoto et al., 2012; Toth et al., 2013). Several factors that restrict synapse formation are present in myelin and glial cells. Nogo-A, myelin-associated glycoprotein, oligodendrocyte glycoprotein, and chondroitin sulfate proteoglycans (CSPGs) converge onto signaling pathways that restrain axon regeneration and neuronal connectivity (Raiker et al., 2010; Delekate et al., 2011; Mironova and Giger, 2013; Zemmar et al., 2014). The reticulon-4 receptor (Nogo-66 receptor or NgR1) is a principal receptor for myelin-associated inhibitors (MAIs) and CSPGs and has been identified as an endogenous negative regulator of synaptic plasticity. NgR1 signaling restricts experience-dependent plasticity in the visual cortex, induces long-term depression and blocks FGF2-mediated LTP in hippocampal slice preparations (McGee et al., 2005; Karlén et al., 2009; Wills et al., 2012; Akbik et al., 2013). Loss of NgR1 expression in hippocampal neurons leads to an increased number of excitatory synapses and impedes dendritic spine maturation. We previously reported a decrease in neuronal sensitivity to MAIs associated with NgR1 surface proteolysis (Ferraro et al., 2011). A lack of metalloproteinase activity could impair excitatory synapse formation by preserving the integrity of inhibitory NgR1 at the synapse.

In the present study, we evaluated the role of MT-MMPs in the development of excitatory synapses. We describe the expression of MT3-MMP, a member of the membrane-bound MMP subfamily, in embryonic and postnatal stages of the cerebral cortex. We find that MT3-MMP loss-of-function reduces excitatory synapse formation *in vitro* and *in vivo*. We find that NgR1 is an MT3-MMP substrate at synapses and that NgR1 is required for MT3-MMP-dependent synapse formation. MT3-MMP activity generates a soluble Ecto-NgR1 (1–358) and a membrane-anchored carboxy-terminal NgR1 (CT-NgR1) fragment during periods associated with excitatory synapse development. Expression of a constitutively shed NgR1 construct or treatment with soluble Ecto-NgR1 (1–358) fragments accelerates excitatory synaptogenesis. Our results demonstrate that MT3-MMP plays an important role in the formation of functional excitatory synapses through regulated NgR1 cleavage.

Materials and Methods

Animals. Timed pregnant [embryonic day (E)18–E19] female Sprague-Dawley and CD1 mice were purchased from Charles River Laboratories. C57BL/6 NgR1-null mice were kindly provided by Dr. Mark Tessier-Lavigne (Stanford University, California). Brain areas were isolated from embryonic (E18) and postnatal days (P)5–P20 (P10–P60) WT CD1 mice. E18, P10, and P60 mice brains were embedded in Tissue-Tek OCT compound and flash frozen with 2-methylbutane. All animal care and use was in accordance with the McGill University guidelines and approved by the University Animal Care and Use Committee. Animals were maintained in standard housing conditions.

Antibodies and reagents. For immunofluorescence, the following antibodies were used: mouse anti-PSD95 (11,000; Millipore), rabbit anti-synapsin-1 (1:1000; Millipore), mouse anti-PSD95 (1:200; NeuroMab), guinea pig anti-VGLUT-1 (1:400; Synaptic Systems), mouse anti-Myc (1:500; Sigma-Aldrich), and goat anti-human IgG Fc (1:500; Jackson ImmunoResearch). AlexaFluor secondary antibodies were purchased from Invitrogen Life Technologies (1:500). For Western blot analysis, the following antibodies were used: goat anti-NgR1 (1:200; R&D Systems); rabbit anti-NgR1 (Dr. Roman Giger, University of Michigan); mouse anti-*N*-Cadherin (1:10,000; M. Takeichi and H. Matsunami, Developmental Studies, Hybridoma Bank); mouse anti-MMP16/MT3 (1:200; Millipore); goat anti-Lingo-1 (1:1000; R&D Systems); mouse anti-synaptophysin (SynPhy; 1:10,000; Sigma-Aldrich); mouse anti-PSD95 (1:100,000; NeuroMab); mouse anti-Myc (1:1000; Sigma-Aldrich); mouse anti-Flag (1:5000; Sigma-Aldrich), and mouse anti-GAPDH (1:200; Santa Cruz Biotechnology). HRP-conjugated secondary antibodies were purchased from Jackson ImmunoResearch.

Primary cell culture. Mouse and rat cortical neuron dissections were described previously (Sanz et al., 2015). Briefly, cortical neurons were prepared from E17–E19. Cerebral cortices were dissected; 0.25% trypsin-EDTA digested; mechanically dissociated and cultured for 14 d on 100 μg/ml poly-L-lysine (Sigma-Aldrich) -coated dishes. Neurons were grown in neurobasal media (Invitrogen) supplemented with 2% B27 (Invitrogen), 1% N2 (Invitrogen), 1% penicillin/streptomycin (Invitrogen), and 1% L-glutamine (Invitrogen). Neuronal culture media were refreshed every 4 d. For immunocytochemical experiments, 8.750×10^3 cells per cm^2 were plated on coverslips. For biochemical experiments, 50×10^3 cells per cm^2 were plated on plastic plates and analyzed at 14 d *in vitro* (DIV).

Plasmids and cloning. Constructs and preparations for soluble human MT1-MMP, lentivirus rat shRNAmir (MT3-MMP and MT5-MMP), WT-NgR1, and constitutively cleaved (CE)-NgR1 were described previously (Morrison and Overall, 2006; Ferraro et al., 2011). The following primers were used to generate mouse shRNAmir for MT3-MMP lentivirus: top: 5′TGCTGTTATCAA GTCATGAGGGTAACGTTTTGGCCAC TGACTGACGTTACCCTTGACTTGATAA′3 and bottom: 5′CCTGTT ATCAAGTCAAGGGTAACGTCAGTCAGTGGCCAAAACGTTACCC TCATGACTTGATAAC′3.

The following primers were used to validate MT3-MMP knockdown in mouse cortical neurons: mouse MT3-FW: 5′CAGCTCTGGAAGAAGGT TGG′3, and mouse MT3-RV: 5′GAGCTGCCT GTCTGGTC′3.

To generate Myc-tagged CT-NgR1 construct, the CT-fragment of human NgR1 was subcloned into a Psectag2B vector by PCR. The IgK-signal sequence and the CT-NgR1 were then subcloned into the pRRL-sinPPT vector by PCR. The following primers were used to generate a Myc-tagged CT-NgR1 fragment: Forward: 5′GAA GGATCCGAACAA AAACTCATCTCAGAAGAGGATCTGCGCGTGCCGCCCGGT′3, Reverse: 5′GAACTCGAGTCAGCAGGGCCCAAGCAC′3.

The following primers were used to subclone the IgK-signal sequence and CT-NgR1 into the pRRL-sinPPT vector: Forward: 5′GGAGGCCG GCCATGGAGACAGACACACTCCTG′3 and reverse: 5′GAACTCGAG CTAGCTACTAGCTAGTCGAGATCTGAGTCCGG′3.

To generate soluble 358-Fc NgR1, the ectodomain of rat NgR1 up to amino acid 358 was subcloned into a Psectag2B vector by PCR. The IgK-signal sequence and the ectodomain of rat NgR1 was then fused to a human Fc segment by subcloning into the PFUSE vector (Invitrogen) at the C-terminal end. The following primers were use to subclone 358-Fc NgR1 into the Psectag2b vector: 358-Fc NgR1 Forward: 5′GCTCAAGC TTCCTGGTGCCTGTGTGTGC′3 and 358-Fc NgR1 Reverse: 5′GCTCGG ATCCTCATTTACCCGGAGACAGG′3. For overexpression experiments *in vivo*, IgK-358-Fc-P2A-eGFP and IgK-Fc-P2A-eGFP sequences were cloned into a pCAG vector from Addgene (11151).

Recombinant protein purification. Generation of Fc-tagged recombinant proteins was described previously (Sanz et al., 2015, 2017). Briefly, HEK293T cells were transfected with calcium phosphate, incubated in OptiMEM (Invitrogen) media, and purified by affinity chromatography with protein A sepharose beads. Protein concentration was estimated by protein assay and visualized by Coomassie-brilliant blue stain next to a BSA curve.

Immunochemistry. For shedding experiments in dissociated neuronal cultures, the culture medium was replaced with neurobasal media and supplemented with pan-metalloproteinase inhibitors: Batimastat (BB-94; 5 μM; Tocris Bioscience), Ilomastat (GM6001; 20 μM; Tocris Bioscience), inactive GM6001 analog (20 μM; Tocris Bioscience), and phospholipase C (PI-PLC; 1U/ml; Invitrogen). After 4–6 h, supernatants were collected and briefly centrifuged to dispose of residual cell debris. Supernatants were concentrated using column centrifuge filters (10K, Amicon Ultra-4, Millipore), resolved on 10% SDS-PAGE gels, and analyzed by Western blot.

Membrane extracts and synaptosome preparations. Cerebral cortices were dissected and homogenized in 1 mM $NaHCO_3$, 0.2 mM $CaCl_2$, and

0.2 mM $MgCl_2$ (homogenization buffer, pH 7.9). All steps were performed at 4°C. Debris was removed by centrifugation at 600 × *g* for 15 min. The supernatant was centrifuged at 25,000 × *g* for 45 min and the pellet was lysed in RIPA lysis buffer.

Synaptosomal preparations were performed as previously described (Lee et al., 2008). Briefly, the cortex was dissected and homogenized in 0.32 M sucrose, 1 mM EDTA, 5 mM Tris, pH 7.4. Buffer was supplemented with Complete-EDTA free protease inhibitor mix (Roche). All steps were performed at 4°C. Homogenate was centrifuged at 1000 × *g* for 15 min. The supernatant (S1 fraction) was overlayed on a Percoll discontinuous gradient, which consisted of the following layers (from top to bottom): 3%, 10%, 15%, and 20% Percoll. Synaptosomes were collected at the 10/15% and 15/20% interfaces and washed twice in homogenization buffer. For shedding experiments, the pellet was resuspended in neurobasal media and incubated with pan-MMP inhibitors. Samples were centrifuged at 20,000 × *g* for 15 min, the pellet was lysed in RIPA buffer, and the supernatant was concentrated with centrifugal filter units (Millipore).

Riboprobe synthesis and in situ *hybridization.* MT-MMP probes were synthesized from mouse cDNA clones of the full coding sequence (Open Biosystems); MT1-MMP (MMM1013-9498156), MT2-MMP (MMM1013-98477873), MT3-MMP (5292478), and MT5-MMP (5687204). Riboprobes were synthesized as described previously (Beaubien and Cloutier, 2009). Briefly, digoxigenin (DIG)-labeled cRNA riboprobes with sense or antisense orientation were synthesized by *in vitro* transcription using DIG labeling mix (Roche) followed by partial hydrolysis with 10 mM DTT, 200 mM $NaHCO_3/Na_2CO_3$, and pH 11. Probed were stored in diethylpyrocarbonate (DEPC)-treated water at −80°C. Fresh frozen brains were cryosectioned at 20 μm at −17°C and thaw mounted on microscope slides (Fisher Scientific). Sections were fixed in 4% paraformaldehyde/0.1 M phosphate-buffered isotonic saline, pH 7.4, then rinsed in PBS and DEPC-treated water. Sections were incubated for 10 min with 0.25% acetic anhydride in 1% triethanolamine, washed twice in PBS, rinsed in 1× standard saline citrate (SSC), and prehybridized for 3 h in 50% formamide, 5× Denhardt's solution, 5× SSC, 200 mg/ml baker's yeast tRNA. Sections were hybridized overnight at 60°C with 100 ng/ml DIG-labeled riboprobe. Sections were washed for in 5× SSC, followed by in 2× SSC, then in 50% formamide containing 0.2× SSC, and finally in 0.2× SSC. Sections were then washed in Tris-buffered saline and blocked for 1 h in a 1% solution of blocking reagent (Roche). Sections were incubated with anti-DIG Fab fragments conjugated to alkaline phosphatase (1:3000) for 3 h followed by washes in TBS. The color reaction was performed overnight at room temperature. Sections were rinsed extensively in PBS and coverslipped with Mowiol 4-88 (Calbiochem). Each *in situ* hybridization experiment was repeated a minimum of three times to eliminate any variability in expression between animals.

Synaptic puncta analysis. For experiments with soluble recombinant treatments, 13 DIV cortical neurons were treated with 5 μg/ml of 358-Fc NgR1 and Fc control construct every 24 h for 2 d. For expression of MT3-MMP and MT5-MMP shRNAmir, cortical neurons 3 DIV were infected with designated lentivirus at a multiplicity of infection (MOI) 10 for 4 h in neurobasal media. For overexpression of WT-NgR1, CE-NgR1, and CT-NgR1, cortical neurons were infected at an MOI of 0.3 or 3. At 14–15 DIV, cortical neurons were fixed in 4% PFA and 20% sucrose in PBS for 30 min. Neurons were blocked in 5% BSA and 0.2% Triton X-100 in PBS solution for 1 h and stained for PSD95 (Millipore), VGLUT1 (Synaptic Systems), or synapsin-1 (Millipore).

Based on previously described methods (Takahashi et al., 2012), all image acquisition, analysis, and quantification were performed in a blinded fashion. Cell culture images were acquired on a confocal microscope, Zeiss 710 using a 40× and 63× oil objective. Images were acquired and prepared for presentation using Adobe Photoshop.

For quantification, cells were stained simultaneously and imaged with identical settings. Synaptic puncta were delineated by the perimeter of the transduced designated neuron. Three dendrites per neuron were randomly selected and the number of synaptic puncta (synapsin-1 or VGLUT1, PSD95, and colocalized synapsin-1 or VGLUT1/PSD95) per 20 μm of dendrite length was measured using the Puncta Analyzer plugin from the ImageJ software. A total of 25–45 cells per condition were analyzed in at least three independent experiments.

In utero *electroporation.* Pregnant mice were deeply anesthetized with isoflurane (4–5% for initial anesthesia, ~2–3% for maintenance). Midline incision was performed through the skin and the abdominal wall to expose the uterine horns. 2 μl of 2.7 μg/μl plasmid mixture (1.8 μg/μl pCAG_MT3-GFP/control-GFP/358-Fc/Fc constructs; 0.9 μg/μl pCAG_Lck-mCherry) were injected into the lateral ventricles of E13–E14 embryos using a glass micropipette. Immediately after injection, five square pulses of current were applied (39–40 V; 50 ms followed by 950 ms intervals) using an electroporator (Harvard Apparatus) and three-pronged tweezer-electrodes. Two electrodes connected to the negative pole were placed on the side of the head with a single positive electrode on the top, above the ventricles. The uterine horns were subsequently replaced in the abdominal cavity. The abdominal cavity was filled with warm PBS, and silk sutures were used to close the overlying abdominal muscle and skin.

Spine counts. Mice were perfused at P24. Brains were collected, fixed with 4% PFA in PBS overnight at 4°C, and immersed consequently in 30% sucrose in PBS at 4°C. The brains were then embedded in OCT compound, and stored at −20°C until analysis. Frozen brains were cut into 40-μm-thick coronal sections by cryostat. Dendritic spines from the cerebral cortex were visualized using a spinning-disc microscope at 100× magnification. Neurons from the layer VI cortex expressing both GFP and Lck-mCherry were randomly selected. 3D spine counts were performed using the NeuronStudio software (Rodriguez et al., 2008). Ten images from 3–5 brains per condition were compiled and analyzed.

Electrophysiological recordings. Cortical neurons were prepared as described previously (Hudmon et al., 2005). Dissociated cortical neurons were plate on poly-D-lysine-coated glass coverslips at a density of 1057 cells/mm^2. Growth media consisted of neurobasal enriched with 1% B27, penicillin/streptomycin (50 U/ml; 50 μg/ml) and 0.5 mM L-glutamax. Fetal bovine serum (5%; Hyclone) was added at the time of plating. After 5 d, half of the media was changed without serum and with Arac-C (5 μM; Sigma-Aldrich). Twice a week thereon, half of the growth medium was replaced with serum and Ara-C–free medium. The neurons were transfected at 8 DIV with Lipofectamine 2000 (Invitrogen) as described previously (Hudmon et al., 2005).

Neurons were continuously perfused (2 ml/min) with aCSF (105 NaCl, 10 HEPES, 10 glucose, 5 KCl, 2 $MgCl_2$, and 1.2 $CaCl_2$, pH 7.3; 235 mOsm/L) using a perfusion system with temperature adjusted to 30–32°C. Whole-cell voltage-clamp recordings were obtained from visually identified transfected cortical cells at 13–15 DIV. For recordings, the glass pipettes of 3.5–5 MΩ were filled with a solution containing the following (in mM): 80 $CsMeSO_3$, 20 CsCl, 10 diNa-phosphocreatine, 10 HEPES, 2.5 $MgCl_2$, 0.6 EGTA, 4 ATP-Tris, 0.4 GTP-Tris, pH 7.28; 215 mOsm/L. mEPSCs were recorded at the reversal potential of GABA (−70 mV) in the presence of tetrodotoxin (0.5 μM; Alomone Labs). Data acquisition (filtered at 1.8 kHz and digitized at 10 kHz) was performed using a MultiClamp 700B amplifier and the Clampex 10.6 software (Molecular Devices). Data were analyzed using Clampfit 10.2 (Molecular Devices) and Igor Pro (Wave Metrics).

Statistics. Analyses were performed using Microsoft Excel and GraphPad Prism5. Statistical comparisons were made using one-way and two-way ANOVA, followed by Bonferroni *post hoc* test and unpaired two-tails *t* test, as indicated in the figure legends. All data are reported as the mean + SEM from at least three independent experiments. Statistical significance was defined as follows: $*p < 0.5$, $**p < 0.01$, and $***p < 0.001$.

Results

MT3-MMP and MT5-MMP are expressed during periods of synaptogenesis

Although MMPs expression has been reported in the CNS, the temporal-spatial expression pattern of MT-MMPs has not been fully described. To evaluate the expression of transmembrane MT-MMPs, we examined the mRNA expression of MT1-MMP, MT2-MMP, MT3-MMP, and MT5-MMP in developing and adult mouse brain by *in situ* hybridization (Fig. 1*a*). The major phase of synaptogenesis occurs during the first month of murine

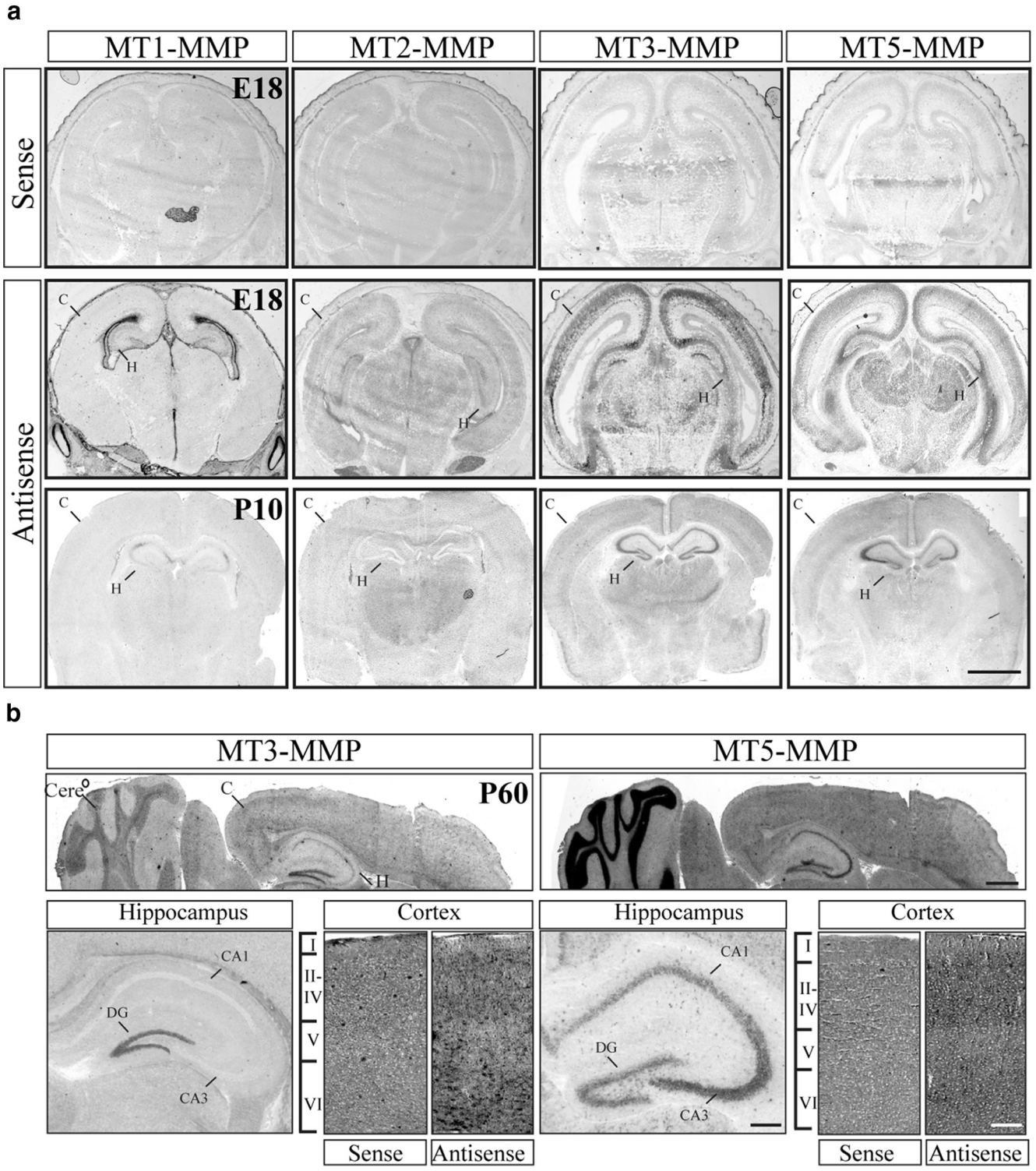

Figure 1. MT3-MMP and MT5-MMP are expressed during periods of synaptogenesis. ***a***, *In situ* hybridization experiment from coronal section of E18 and early P10 mouse cerebrum with antisense cRNA probes for members of the MT-MMP subfamily (MT1-MMP, MT2-MMP, MT3-MMP, and MT5-MMP). ***b***, Sagittal sections from mouse cerebrum at P60, probed for MT3-MMP and MT5-MMP expression. Mouse cerebral areas from P60 hippocampus and cerebral cortex, probed for MT3-MMP and MT5-MMP mRNA expression. H, Hippocampus; c, cortex. The expression of MT-MMPs was assessed in three independent brains from developmental stages (E18, P10, and P60). The ability of MT-MMP probes was validated by comparison to sense control probes. Scale bar, 1 mm.

life (P5–P35), peaking at the second postnatal week (Herschkowitz et al., 1997). Before synapse formation at E18, robust expression of MT3-MMP and MT5-MMP is detected in the cortex and hippocampus, whereas MT2-MMP and MT1-MMP are weak or absent (Fig. 1*a*; Huttenlocher, 1979). At P10, when synapses begin to abruptly increase in density, MT3-MMP and MT5-MMP are expressed by neurons in layers II–IV and layer VI of the cerebral cortex and in areas CA1/CA3 and dentate gyrus (DG) of the hippocampus, suggesting a role in neuronal connectivity. Following synapse formation, neuronal networks undergo continu-

ous remodeling of synaptic connections, possibly through focal expression and activity of metalloproteinases (Nudo et al., 1996; Fu and Zuo, 2011). Interestingly at P60, MT3-MMP and MT5-MMP are highly present in regions of synaptic plasticity. MT5-MMP is expressed in the granular layer of the cerebellum and the CA1/CA3 and DG of the hippocampus, whereas MT3-MMP is specifically enriched in the DG. Similarly, MT3-MMP and MT5-MMP are expressed in most cortical layers, except for layers I and V (Fig. 1*b*). Together, we conclude that MT3-MMP and MT5-MMP expressions correlate with the process of synaptogenesis and are maintained in regions that exhibit high levels of synaptic plasticity.

MT3-MMP loss-of-function decreases excitatory synapse formation

Based upon the expression pattern of MT-MMPs, we evaluated their contribution to synaptogenesis by examining the number of excitatory synapses in mature dissociated cortical neurons following MT-MMP inhibition by the pan-metalloproteinase inhibitor, BB-94. Syn-1 and PSD95 puncta were used to delineate presynaptic and postsynaptic sites and their overlap used to detect putative excitatory synapses. Treatment with BB-94 significantly decreased the levels of Syn-1 by 43.4%, PSD95 by 27.3% and colocalized puncta by 47.8% at day 14, signifying that metalloproteinases promote excitatory synaptogenesis (Fig. 2*a*,*b*). To specifically investigate the effects of MT3-MMP and MT5-MMP on excitatory synapses, we knocked down MT3-MMP and MT5-MMP expression using shRNAs introduced into a microRNA backbone (shRNAmir; Fig. 2*c*–*f*). Knockdown of MT3-MMP, but not MT5-MMP, repressed synapse formation similar to BB-94. Following MT3-MMP knockdown levels of Syn-1 decreased by 31.1%, PSD95 by 45.1% and colocalized Syn-1/PSD95 puncta by 56.8% (Fig. 2*f*). Consistent with loss of synapses detected by immunolabeling, electrophysiological recordings revealed that loss of MT3-MMP activity significantly decreased the frequency of miniature EPSCs (mEPSCs), with no effect on the mEPSC amplitude (Fig. 2*g*,*h*). Thus, MT3-MMP promotes the formation of functional excitatory synapses.

MT3-MMP loss-of-function inhibits synapse and spine formation *in vivo*

MT-MMPs are constitutively expressed in many tissues and are implicated in a wide range of physiological and pathological processes. To explore the neuronal cell autonomous function of MT3-MMP in excitatory synaptogenesis *in vivo*, we knockdown the expression of MT3-MMP by *in utero* electroporation (Fig. 3*a*,*b*). Based upon the expression pattern of MT-MMPs (Fig. 1), we electroporated MT3-MMP shRNAmir in the mouse brain at E13 and quantified the number of dendritic spines in layers III and VI of the cerebral cortex (Fig. 3*c*,*d*). At P24, the loss of MT3-MMP activity significantly decreased the density of dendritic spines in both cortical layers (Fig. 3*d*,*e*), demonstrating that neuronally expressed MT3-MMP enhances the number of excitatory synapses *in vivo*.

MT3-MMP mediates synaptic NgR1 shedding

NgR1 is an endogenous repressor of synaptogenesis and synaptic plasticity. Overexpression of MT1-MMP, MT3-MMP, and MT5-MMP are able to cleave the ectodomain of NgR1 relieving myelin-dependent outgrowth inhibition (Ferraro et al., 2011). In loss-of-function experiments in healthy cortical neurons, MT3-MMP mediates endogenous NgR1 shedding (Ferraro et al., 2011). We therefore asked whether NgR1 is a synaptic MT3-MMP substrate that is shed to alleviate the repressive effect of NgR1 on excitatory synapse formation. NgR1 shedding generates two fragments, a soluble shed 50 kDa fragment and a 30 kDa fragment that remains anchored to the cell surface by the GPI moiety (CT-NgR1; Fig. 4*a*). We used an antibody that specifically detects both FL-NgR1 and CT-NgR1 in crude membrane extracts and validated its specificity by demonstrating a loss of reactivity in samples from NgR1 knock-out mice (Fig. 4*b*). By treating cortical neurons with recombinant MT1-MMP to cleave NgR1 and performing cell surface biotinylation, we demonstrated an increase in CT-NgR1 levels at the expense of FL-NgR1 with this antibody (Fig. 4*c*). More detailed characterization of NgR1 shedding from P5 to P30 cerebral cortices showed a progressive increase in the CT-NgR1 band that increases from P10 to P30, during the peak of synapse formation (Fig. 4*d*,*e*). This accumulation of CT-NgR1 mirrored the expression of the excitatory postsynaptic marker PSD95, supporting a potential relationship between NgR1 shedding and excitatory synapse development (Fig. 4*d*).

We then assessed expression of NgR1 and MT3-MMP in synaptosomes isolated from the mature cerebral cortex and separated into extra-synaptic, presynaptic and postsynaptic fractions (Fig. 4*f*). Consistent with previous reports FL-NgR1 was present in all synaptic subdomains, with highest expression in extrasynaptic and postsynaptic subfractions (Fig. 4*f*; Lee et al., 2008). The CT-NgR1 fragment is strongly enriched in the postsynaptic subfraction, suggesting that it is cleaved on the postsynaptic membrane. MT3-MMP is present in all synaptosome subfractions and is enriched in extrasynaptic and postsynaptic compartments. To directly assess NgR1 shedding, we probed conditioned media from isolated synaptosomes. A 50 kDa NgR1 fragment was detected in the conditioned media and treatment of synaptosomes with pan-metalloproteinase inhibitors, BB-94 or GM6001, blocked the release of the NgR1 ectodomain fragment (Fig. 4*g*). The NgR1 shedding profile is similar to *N*-Cadherin, a previously identified metalloproteinase substrate (Fig. 4*g*). To test whether MT3-MMP mediates synaptic NgR1 cleavage, we performed shedding experiments from dissociated 14 DIV cortical neurons expressing MT3-MMP shRNAmir and assessed NgR1 ectodomain levels in the conditioned media (Fig. 4*h*,*i*). Knockdown of MT3-MMP expression, but not MT5-MMP as a control, significantly decreased the levels of NgR1 shed fragment by 61.4% (Fig. 4*i*). Together, we conclude that MT3-MMP is responsible for synaptic NgR1 shedding from cortical neurons and that NgR1 is primarily cleaved on the postsynaptic membrane to release a soluble fragment.

NgR1 shedding is sufficient to promote excitatory synapse formation

Previously, we reported that MT-MMPs decrease neuronal sensitivity to soluble MAI by diminishing NgR1 surface levels (Ferraro et al., 2011). Furthermore, NgR1 shed fragment retains the ability to bind Nogo-66, suggesting a dominant-negative function for NgR1 cleavage fragment (Walmsley et al., 2004). To assess the contribution of NgR1 proteolysis in excitatory synapse formation, we examined the number of excitatory puncta in neurons overexpressing WT-NgR1 or a previously characterized NgR1 mutant with enhanced cleavage (cleavage-enhanced, CE-NgR1; Ferraro et al., 2011). At a low MOI, WT-NgR1 dampens the number of excitatory synapses, as previously reported (Fig. 5*a*,*b*; Wills et al., 2012). We also found that the anti-synaptogenic effect of WT-NgR1 disappeared when neurons were transduced with a high viral titer and we noted that this was accompanied by an increased deposition of NgR1 cleaved fragment in the synaptic

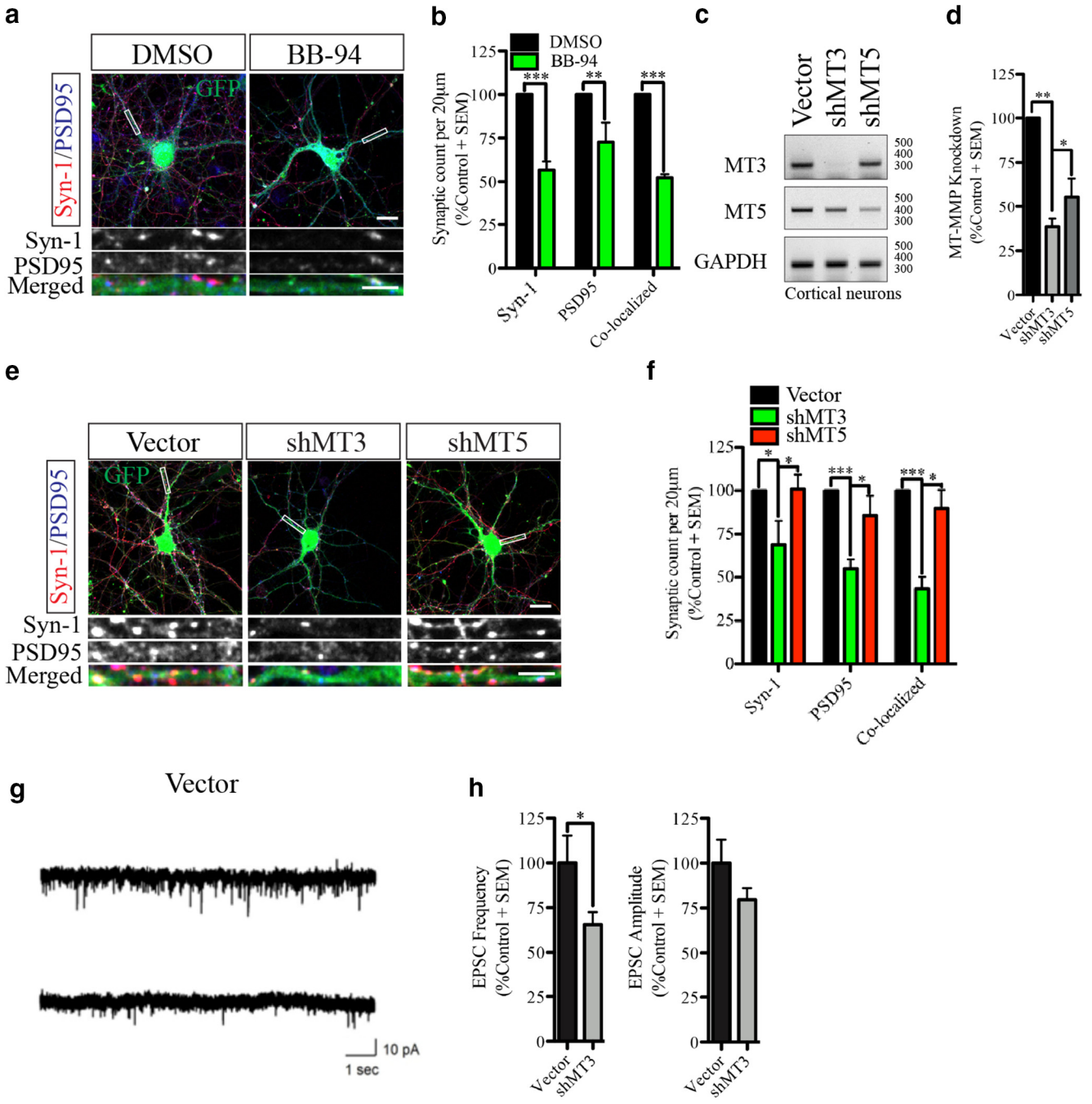

Figure 2. MT3-MMP loss-of-function decreases excitatory synapse formation. ***a***, Fourteen days *in vitro* cortical neurons infected with a control lentivirus and treated with DMSO or BB-94 for 7 d. ***b***, Synaptic counts from DMSO and BB-94-treated cortical neurons stained for Syn-1 and PSD95. ***c***, ***d***, RT-PCR from rat cortical neurons 14 DIV infected with a lentivirus encoding MT3-MMP shRNAmir, MT5-MMP shRNAmir, or a control empty vector. GAPDH was used as a loading control. ***e***, Cortical neurons 14 DIV infected with a lentivirus encoding MT3-MMP shRNAmir, MT5-MMP shRNAmir, or a control empty vector. ***f***, Synaptic counts from MT3-MMP and MT5-MMP knockdown experiments in cortical neurons stained for Syn-1 and PSD95. ***g***, ***h***, Representative examples of whole-cell patch-clamp recordings from cortical neurons expressing MT3-MMP shRNAmir or control condition (***g***). mEPSCs recorded from dissociated cortical neurons expressing MT3-MMP shRNAmir (***h***). Scale bars: 12 (upper panel ***a*** and ***e***) and 4 (lower panel ***a*** and ***e***). $*p < 0.5$, $**p < 0.01$, $***p < 0.001$.

conditioned media (Fig. 5*a*,*b*). We reasoned that this fragment may neutralize the anti-synaptogenic effect of NgR1. To test this possibility, we infected neurons with a previously reported NgR1 mutant with enhanced cleavage. Synaptic counts were performed in neurons expressing CE-NgR1 (Fig. 5*a*,*c*). Low-level transduction with CE-NgR1 were sufficient to generate shed NgR1 in the conditioned media and this construct failed to suppress synapse formation (Fig. 5*a*,*c*). High levels of CE-NgR1 expression were sufficient to mediate strong NgR1 cleavage in the cultures (Fig. 5*a*) and this was accompanied by a significant increase in Syn-1 puncta (61.6%), PSD95 puncta (58.8%), and colocalized puncta (70.7%; Fig. 5*c*). Furthermore, the presence of a pan-metalloproteinase inhibitor decreased the number of excitatory synapses in CE-NgR1 transduced neurons, implicating metalloproteinase activity in excitatory synapse potentiation by CE-NgR1 (Fig. 5*d*,*e*). Together this supports a role for MT3-MMP in promoting excitatory synapses through regulated surface NgR1 proteolysis.

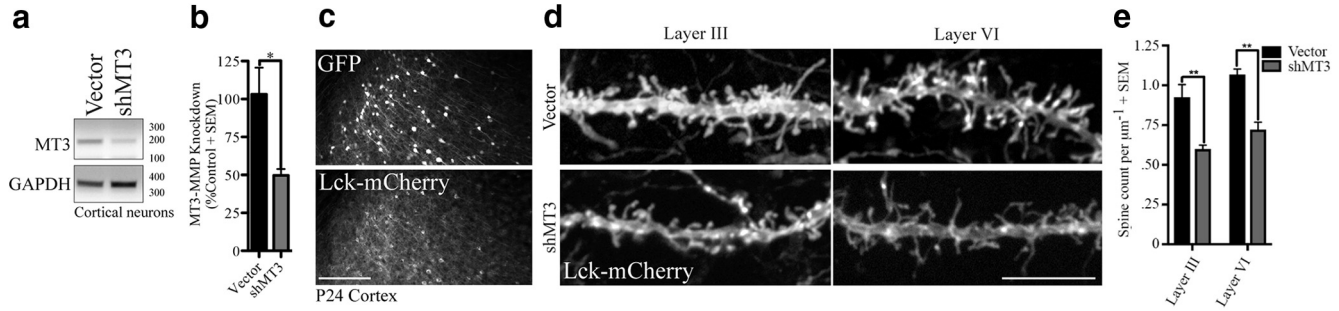

Figure 3. MT3-MMP loss-of-function decreases dendritic spines *in vivo*. ***a***, ***b***, RT-PCR analysis from mouse cortical neurons infected with control empty vector or MT3-MMP shRNAmir. ***c***, Coronal sections of mouse brain *in utero* coelectroporated with control GFP or MT3-MMP shRNAmir and Lck-mCherry. ***d***, Dendritic spines in layers III and VI of the cerebral cortex *in utero* coelectroporated with control GFP or MT3-MMP shRNAmir and Lck-mCherry. ***e***, Number of dendritic spines in layers III and VI of the cerebral cortex, expressing MT3-MMP shRNAmir or GFP control by *in utero* electroporation. One hundred dendrites from three to five independent brains. Scale bars: 500 (c) and 5 (d) μm. Data are mean + SEM. *$p < 0.05$, **$p < 0.01$ by Bonferroni *post hoc* test.

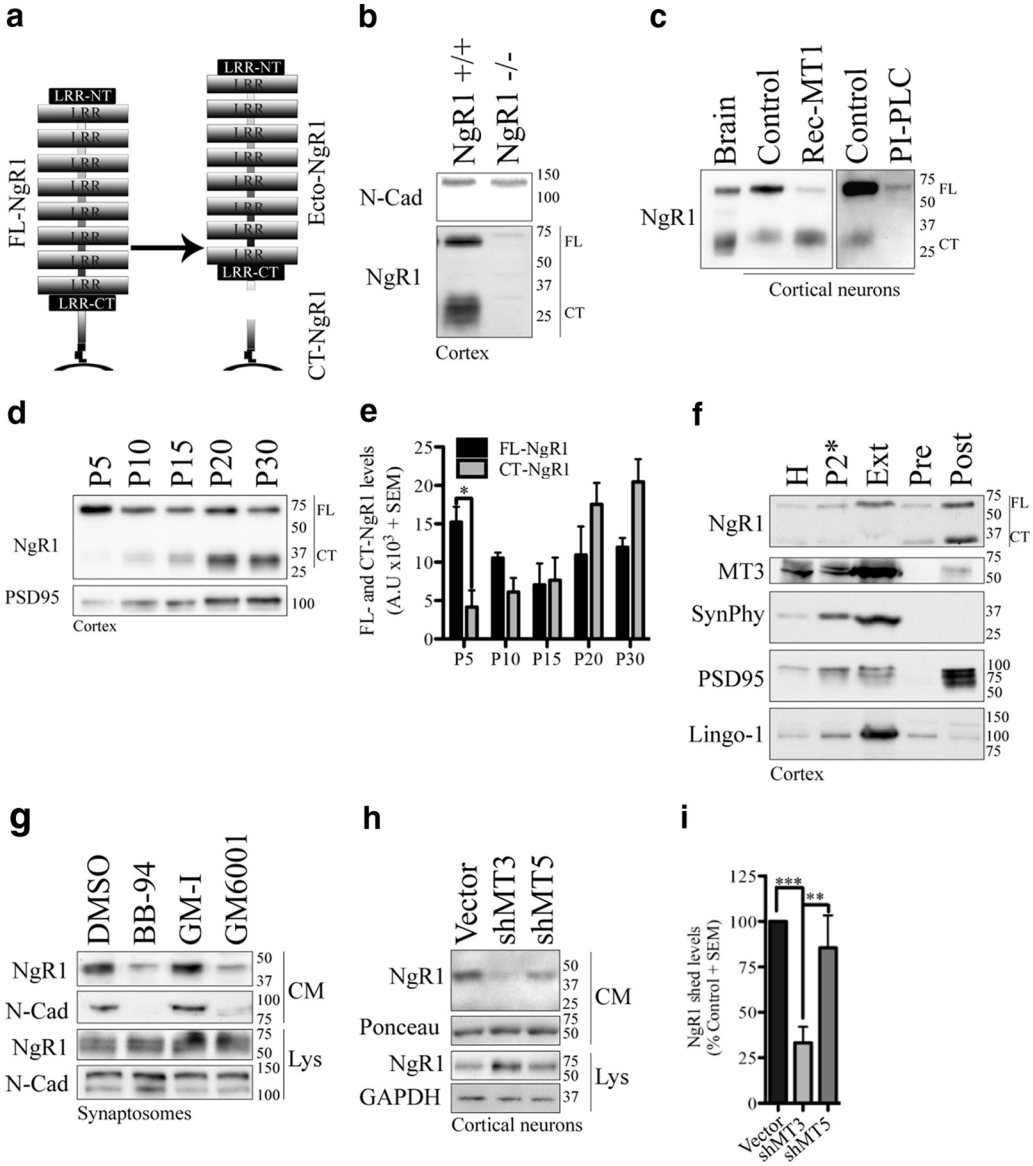

Figure 4. MT3-MMP mediates synaptic NgR1 shedding from cortical neurons. ***a***, Schematic representation of soluble Ecto-NgR1 (1–358) and CT-NgR1 (359–410) fragments generated by surface NgR1 proteolysis. ***b***, Crude membrane extract from WT and NgR1-KO mice probed with commercially available mouse anti-NgR1 polyclonal antibody. ***c***, Cell-surface biotinylation of mouse dissociated cortical neurons treated with 0.75 μM rec-MT1-MMP and PI-PLC, probed with commercially available mouse anti-NgR1 polyclonal antibody. ***d***, Membrane extracts from mouse cerebral cortex (P10–P30) probed for NgR1 and PSD95. ***e***, Densitometry analysis of full-length NgR1 and CT-NgR1 during cortical mouse development. ***f***, Synaptosomes from mouse cerebral cortex fractionated into extrasynaptic (Extra), presynaptic (Pre) and postsynaptic (Post) compartments. PSD95, SynPhy, and Lingo-1 were used as markers for synaptic subfractions. ***g***, Conditioned media and lysates from cortical synaptosomes treated with pan-metalloprotease inhibitors, BB-94 and GM6001, DMSO, and GM6001-inactive control (GM-I). *N*-Cadherin (*N*-Cad) expression in media and lysates was used as a control MMP-substrate. ***h***, ***i***, NgR1 shed fragments in the conditioned media and quantification (protein densitometry) from MT3-MMP and MT5-MMP knockdowns in cortical neurons aged for 14 DIV. $N = 3–7$ from independent brains, or dissociated cortical cultures. Data are mean + SEM. *$p < 0.05$, **$p < 0.01$, ***$p < 0.001$, by Bonferroni *post hoc* test.

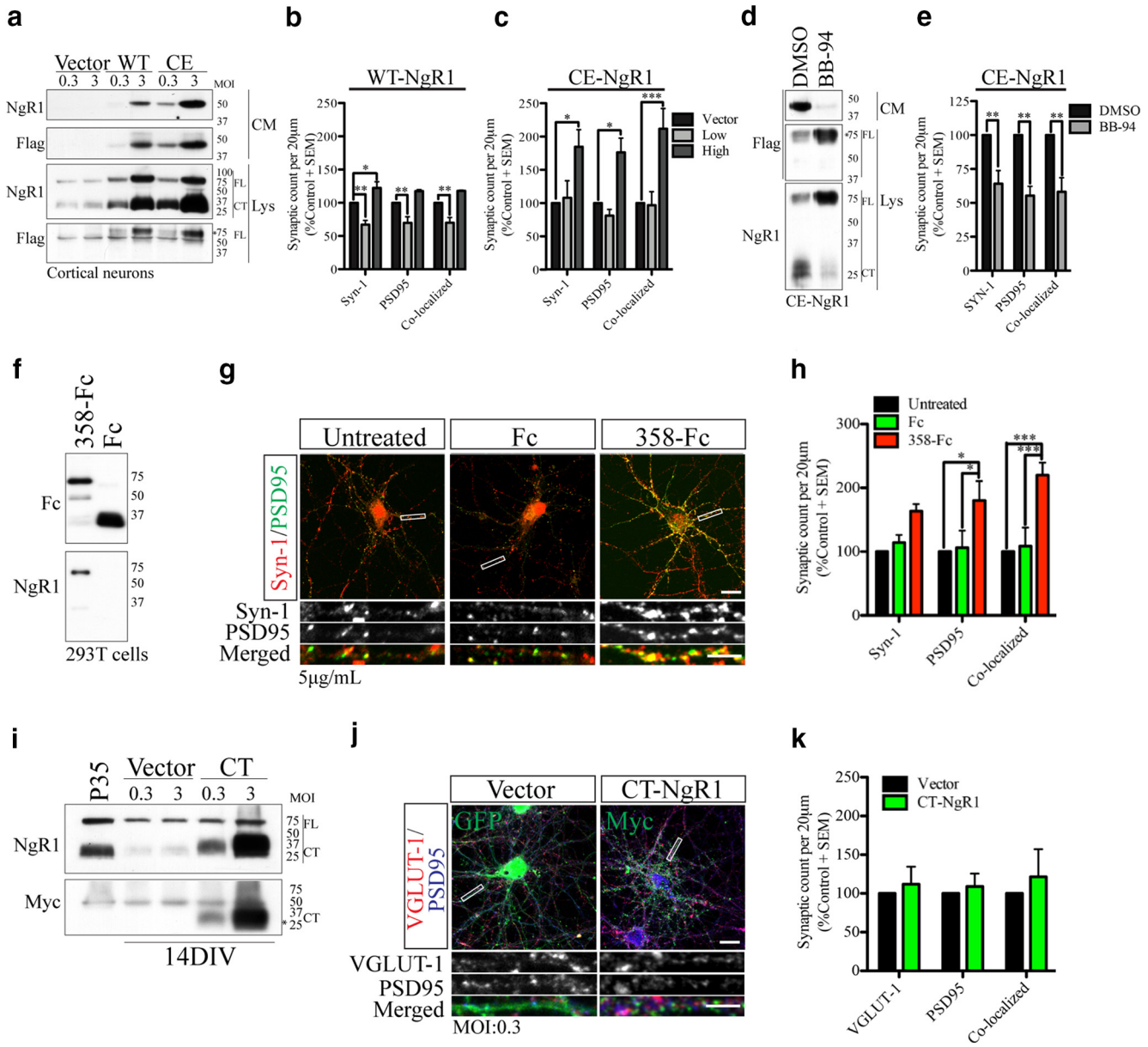

Figure 5. NgR1 shedding and Ecto-NgR1 (1–358) fragment are sufficient to promote excitatory synapses. ***a***, Lysates and conditioned media from cortical neurons expressing WT-NgR1 and CE-NgR1 at different MOI (0.3 and 3). ***b***, ***c***, Synaptic counts from cortical neurons overexpressing WT and CE-NgR1 at MOI 0.3 and 3 and stained for Syn-1 and PSD95. Synaptic counts were normalized to corresponding vector control. ***d***, Lysates from cortical neurons expressing CE-NgR1 and exposed to BB-94. ***e***, Synaptic counts from cortical neurons overexpressing CE-NgR1 in the presence or absence of BB-94. Synaptic counts were normalized to DMSO control. $N = 3–4$ from independent cultures. ***f***, Recombinant Fc and 358-Fc generated in Hek293T cells. ***g***, Cortical neurons aged for 14 DIV and treated with soluble 358-Fc or Fc control every 24 h for 2 d. ***h***, Synaptic counts for cortical neurons treated with recombinant proteins for 48 h and stained for Syn-1 and PSD95. ***i***, Lysates from cortical neurons expressing CT-NgR1 at different MOI. ***j***, Cortical neurons infected with lentivirus encoding CT-NgR1 or empty vector at MOI 0.3. ***k***, Synaptic counts from cortical neurons overexpressing CT-NgR1 stained for VGLUT-1 and PSD95. Synaptic counts were normalized to corresponding vector control. $N = 4$ from independent cultures. Data are mean + SEM. $^*p < 0.05$, $^{**}p < 0.01$, $^{***}p < 0.001$ by Bonferroni *post hoc* test. Scale bars: 12 (upper panel g and j) and 4 (lower panel g and j) μm.

As a parallel approach, we exposed cortical neurons to the recombinant shed ecto-domain of NgR1, Ecto-NgR1 (1–358) fused to the Fc region of human IgG (Fig. 5*f*). Similar to CE-NgR1, Ecto-NgR1 (358-Fc) increases Syn-1 by 54.5%, PSD95 by 60% and Syn-1/PSD95 colocalized puncta by 73.3%, demonstrating that the soluble NgR1 cleaved fragment is sufficient to enhance excitatory synapse formation (Fig. 5*g*,*h*). Overexpression of the 30 kDa C-terminal stub of NgR1 that is retained on the cell membrane (CT-NgR1) after NgR1 shedding, did not affect the formation of excitatory synapses (Fig. 5*i*–*k*).

The NgR1 Ectodomain cleavage fragment promotes excitatory synapse formation *in vivo*

To evaluate the ability of the cleaved NgR1 fragment to promote excitatory synapse formation *in vivo*, we electroporated E13 mice to overexpress soluble 358-Fc and Fc control (Fig. 6*a*) and assessed dendritic spine formation in layers III and VI of the cerebral cortex (Fig. 6*b*,*c*). At P14, secretion of 358-Fc significantly increases the number of dendritic spines in layers III and VI of the cerebral cortex compared with Fc control demonstrating that the shed fragment of NgR1 is sufficient to promote excitatory synapse formation *in vivo* (Fig. 6*c*).

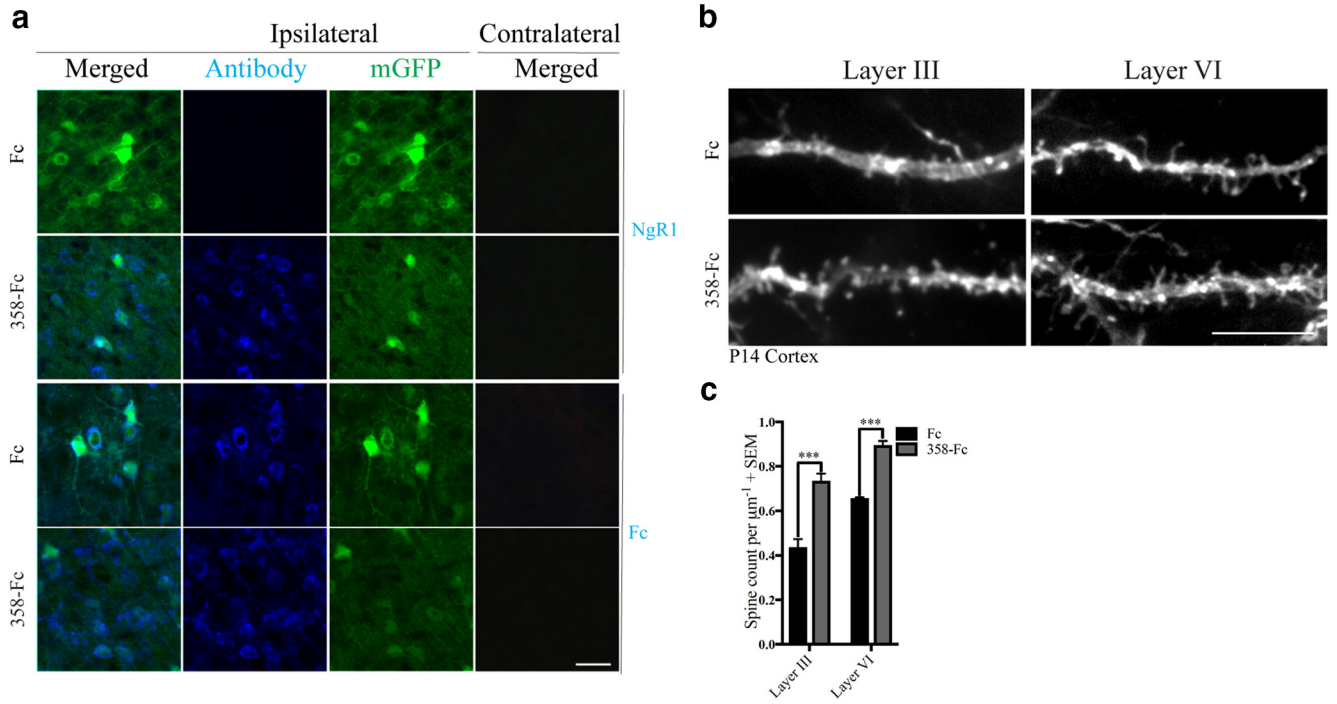

Figure 6. The shed NgR1 ectodomain fragment promotes excitatory synapse formation *in vivo*. ***a***, Coronal sections of mouse brain *in utero* electroporated with control Fc or 358-Fc. Ipsilateral (Ipsi) and Contralateral (Contra) sections stained with an anti-human Fc or anti-NgR1 antibody to validate the constructs. ***b***, Representative images of dendritic spines present in layers III and VI cerebral cortex from mice *in utero* electroporated with 358-Fc or Fc constructs. ***c***, Number of dendritic spines in layers III and VI of mouse cerebral cortex electroporated with Fc or 358-Fc. Sixty dendrites from three independent brains. Scale bars: 50 (a) and 5 (b) μm. Data are mean + SEM. ***$p < 0.001$ by Bonferroni *post hoc* test.

MT3-MMP effects on excitatory synapse formation are dependent on NgR1

To directly test whether the prosynaptogenic effects of MT3-MMP can be fully attributed to its effect on NgR1 shedding, we suppressed MT3-MMP expression in neurons from NgR1-null mice and quantified the number of excitatory synapses (Fig. 7*a*,*b*). Unlike wild-type mice, in an NgR1-null background, loss of MT3-MMP activity failed to inhibit excitatory synaptogenesis with no effect on the number of Syn-1, PSD95, or Syn-1/PSD95-positive punctae (Fig. 7*b*). We then evaluated the ability of Ecto-NgR1 fragment to rescue excitatory synapse development in the absence of MT3-MMP activity (Fig. 7*c*,*d*). Exposure of dissociated cortical neurons expressing MT3-MMP shRNAmir to Ecto-NgR1 (358-Fc) rescues the number of Syn-1, PSD-95, and colocalized punctae. We conclude that NgR1 cleavage can rescue the formation of excitatory synapses in the absence of MT3-MMP activity. Together the data supports a model whereby MT3-MMP-dependent shedding of NgR1 plays a key role in the formation of excitatory cortical synapses (Fig. 7*e*).

Discussion

Several lines of evidence have suggested a role for metalloproteinases in structural remodelling of synaptic networks. Metalloproteinase expression and activity is observed in close opposition to molecular markers of excitatory postsynaptic scaffolding and presynaptic vesicle proteins (Wilczynski et al., 2008). Furthermore, many constituents of synaptic connections are targeted by metalloproteinases, implying their importance in synaptic circuit remodeling. In the present study, we evaluated the role of membrane-type metalloproteinases in excitatory synapse development. Through *in situ* hybridization, we identified two members of the MT-MMP subfamily, MT3-MMP, and MT5-MMP, abundantly expressed in the developing and mature cerebral cortex (Fig. 1). MT5-MMP has previously been reported to localize to synapses through interactions with proteins containing PDZ domains and the glutamate receptor interacting protein, suggesting a function for MT-MMPs in synaptogenesis (Monea et al., 2006). Interestingly, loss of MT3-MMP activity, but not MT5-MMP, restricted the number of excitatory synapses in dissociated cortical neurons and decreased the frequency of mEPSCs (Fig. 2). Similar to MMP-9, a well characterized metalloproteinase important for synaptic physiology and plasticity (Monea et al., 2006), the loss of MT3-MMP expression decreased the density of dendritic spines *in vivo* (Fig. 3), implying a new function for MT3-MMP in excitatory synapse development.

Previously, we reported a role for metalloproteinases in the processing of surface NgR1 (Ferraro et al., 2011). NgR1 is an endogenous repressor of synaptic plasticity that gradually increases in expression in the neonatal brain, inhibits the formation of excitatory synapses and the turnover of dendritic spines (Lee et al., 2008; Wills et al., 2012; Akbik et al., 2013). MT3-MMP might have a prosynaptic effect by targeting synaptic NgR1 protein. We identified MT3-MMP as the major sheddase for synaptic NgR1 at baseline levels in cortical neurons. MT3-MMP is present in synaptosomes and colocalizes with NgR1 cleave fragment (Fig. 4). Loss of MT3-MMP activity decreases NgR1 shedding in dissociated cortical neurons (Fig. 4). Furthermore, the absence of MT3-MMP activity inhibits excitatory synapse formation only in the presence of NgR1 (Fig. 6), implying NgR1 as the downstream effector of MT3-MMP-dependent proteolysis important for excitatory synapse development. Accordingly, ectopic expression of a constitutively cleaved NgR1 (CE-NgR1) construct and treatment with Ecto-NgR1 (1–358) are sufficient to accelerate excitatory synaptogenesis (Figs. 5, 7). Therefore, we propose that

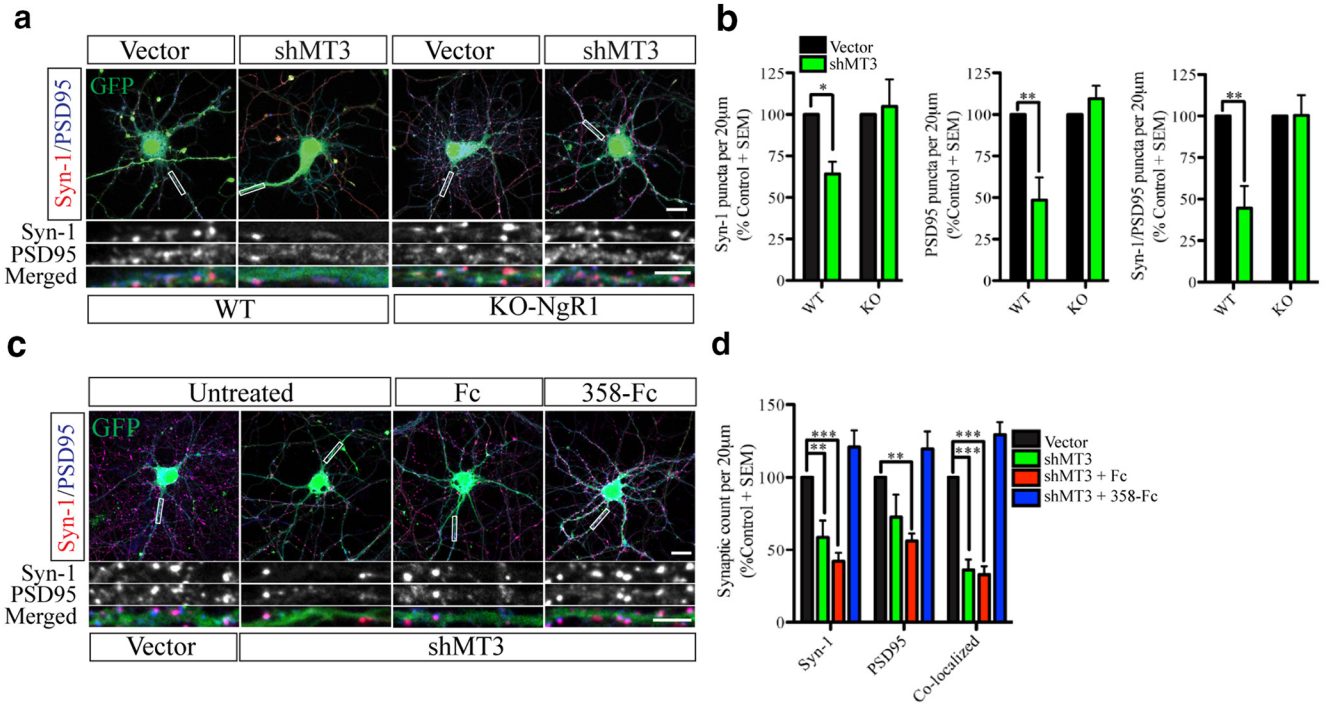

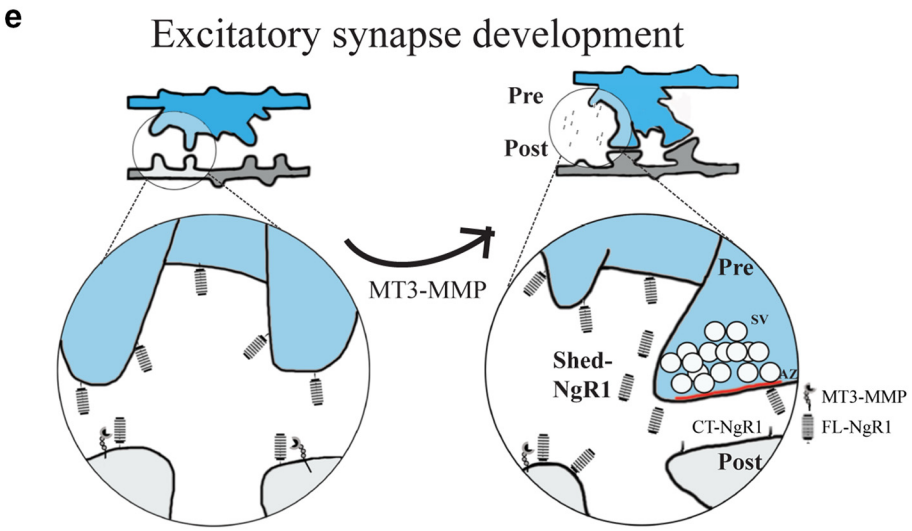

Figure 7. MT3-MMP effects on excitatory synapse formation are dependent on NgR1. ***a***, Cortical neurons from WT or NgR1-deficient mice infected with control empty vector or MT3-MMP shRNAmir. ***b***, Synaptic counts from MT3-MMP knockdown experiments in WT and NgR1-null cortical neurons. Synaptic counts were normalized to corresponding vector control. ***c***, Cortical neurons from WT mice infected with control empty vector or MT3-MMP shRNAmir and exposed to soluble 358-Fc or Fc control at 7 and 14 DIV. ***d***, Synaptic counts from MT3-MMP knockdown experiments in WT cortical neurons. Synaptic counts were normalized to corresponding vector control. All data corresponds to $N = 3–4$ from independent cortical cultures. Data are mean + SEM. $^{*}p < 0.05$, $^{**}p < 0.01$, $^{***}p < 0.001$, by Bonferroni *post hoc* test. Scale bars: 12 (upper panel a and c) and 4 (lower panel a and c) μm. ***e***, Model for MT3-MMP and NgR1 shedding in excitatory synaptogenesis. Cortical neurons express FL-NgR1 in the extrasynaptic, presynaptic, and postsynaptic terminal subdomains. FL-NgR1 is processed by MT3-MMP activity, releasing an ecto-NgR1 fragment (1–358) into the pericellular microenvironment. Surface FL-NgR1 proteolysis and release of Ecto-NgR1 (1–358) promote the formation of excitatory synapses.

NgR1 shed fragment might be acting as a dominant-negative entity to attenuate inhibitory cues in the synaptic environment and promote excitatory synaptogenesis.

NgR1 has recently been described as a molecular-brake that titrates synaptic plasticity and is responsible for the repressive adult-like state in the brain connectivity (Lee et al., 2008; Wills et al., 2012; Akbik et al., 2013). Furthermore, NgR1 restricts surface trafficking of AMPA receptors in the barrel cortex (Jitsuki et al., 2016), illustrating a potential role for NgR1 in limiting the strength of synaptic communication. Interestingly, NgR1 shedding is present during postnatal development and in the mature cerebral cortex (Fig. 4), implying its importance in ongoing cognitive processes. Surface NgR1 expression might be important for the stability of neuronal networks, while NgR1 shedding might provide a permissive microenvironment to facilitate changes in synaptic strength, morphology and density that continue to appear throughout life (Florence et al., 1998; Fu and Zuo, 2011). It remains to be determined whether synaptic activity triggers MT3-MMP expression and NgR1 shedding. Previous groups have reported synaptic activity to downregulate NgR1 expression at the mRNA and protein level (Wills et al., 2012; Karlsson et al., 2013). Glutamatergic receptors, intracellular calcium, as well as Ca^{+2}/

calmodulin-dependent protein kinase II (CaMKII) activity have been reported to promote trafficking and activation of metalloproteinases (Peixoto et al., 2012; Suzuki et al., 2012; Toth et al., 2013). In addition, metalloproteinase expression is upregulated in response to sensory deprivation and damage to the brain circuitry. ADAM-10 and MT5-MMP increase synaptic expression in response to traumatic brain injury (Warren et al., 2012), while rapid changes in ECM composition following monocular deprivation are inhibited in MMP-9-deficient mice (Kelly et al., 2015). Therefore, focal expression and activity of MT3-MMP might increase NgR1 proteolysis to promote plasticity during periods of synaptic activity.

Several groups have targeted the NgR1 signaling pathway as a potential strategy to promote synaptic plasticity. Functional blocking antibodies against Nogo-A and NgR1 promote spine formation and LTP in organotypic slice cultures from the cerebral cortex (Zemmar et al., 2014). Recently, delivery of (1–310) Ecto-NgR1 fragment was shown to promote erasure of fear memories by increasing plasticity of inhibitory synaptic connections (Bhagat et al., 2016). Furthermore, a soluble ecto-domain fragment of paired-Ig-like receptor B increases visual acuity and spine density in mice following long-term monocular deprivation (Bochner et al., 2014). Here, we report that NgR1 proteolysis is an endogenous mechanism necessary for excitatory synapse development that promotes excitatory synapse formation both *in vitro* and *in vivo*. MT3-MMP activity or Ecto-NgR1 (1–358) fragments could enhance circuitry remodelling during development, as well as during cognitive processes in the adult brain.

References

Akbik FV, Bhagat SM, Patel PR, Cafferty WB, Strittmatter SM (2013) Anatomical plasticity of adult brain is titrated by Nogo receptor 1. Neuron 77:859–866. CrossRef Medline

Beaubien F, Cloutier JF (2009) Differential expression of SliTrk family members in the mouse nervous system. Dev Dyn 238:3285–3296. CrossRef Medline

Bhagat SM, Butler SS, Taylor JR, McEwen BS, Strittmatter SM (2016) Erasure of fear memories is prevented by Nogo receptor 1 in adulthood. Mol Psychiatry 21:1281–1289. CrossRef Medline

Bochner DN, Sapp RW, Adelson JD, Zhang S, Lee H, Djurisic M, Syken J, Dan Y, Shatz CJ (2014) Blocking PirB up-regulates spines and functional synapses to unlock visual cortical plasticity and facilitate recovery from amblyopia. Sci Transl Med 6:258ra140. CrossRef Medline

Delekate A, Zagrebelsky M, Kramer S, Schwab ME, Korte M (2011) NogoA restricts synaptic plasticity in the adult hippocampus on a fast time scale. Proc Natl Acad Sci U S A 108:2569–2574. CrossRef Medline

Dityatev A, Schachner M (2003) Extracellular matrix molecules and synaptic plasticity. Nat Rev Neurosci 4:456–468. CrossRef Medline

Ferraro GB, Morrison CJ, Overall CM, Strittmatter SM, Fournier AE (2011) Membrane-type matrix metalloproteinase-3 regulates neuronal responsiveness to myelin through Nogo-66 receptor 1 cleavage. J Biol Chem 286:31418–31424. CrossRef Medline

Florence SL, Taub HB, Kaas JH (1998) Large-scale sprouting of cortical connections after peripheral injury in adult macaque monkeys. Science 282:1117–1121. CrossRef Medline

Fu M, Zuo Y (2011) Experience-dependent structural plasticity in the cortex. Trends Neurosci 34:177–187. CrossRef Medline

Gundelfinger ED, Frischknecht R, Choquet D, Heine M (2010) Converting juvenile into adult plasticity: a role for the brain's extracellular matrix. Eur J Neurosci 31:2156–2165. CrossRef Medline

Herschkowitz N, Kagan J, Zilles K (1997) Neurobiological bases of behavioral development in the first year. Neuropediatrics 28:296–306. CrossRef Medline

Hudmon A, Lebel E, Roy H, Sik A, Schulman H, Waxham MN, De Koninck P (2005) A mechanism for Ca^{2+}/calmodulin-dependent protein kinase II clustering at synaptic and nonsynaptic sites based on self-association. J Neurosci 25:6971–6983. CrossRef Medline

Huttenlocher PR (1979) Synaptic density in human frontal cortex: developmental changes and effects of aging. Brain Res 163:195–205. CrossRef Medline

Jitsuki S, Nakajima W, Takemoto K, Sano A, Tada H, Takahashi-Jitsuki A, Takahashi T (2016) Nogo receptor signaling restricts adult neural plasticity by limiting synaptic AMPA receptor delivery. Cereb Cortex 26:427–439. CrossRef Medline

Karlén A, Karlsson TE, Mattsson A, Lundströmer K, Codeluppi S, Pham TM, Bäckman CM, Ogren SO, Aberg E, Hoffman AF, Sherling MA, Lupica CR, Hoffer BJ, Spenger C, Josephson A, Brené S, Olson L (2009) Nogo receptor 1 regulates formation of lasting memories. Proc Natl Acad Sci U S A 106:20476–20481. CrossRef Medline

Karlsson TE, Koczy J, Brené S, Olson L, Josephson A (2013) Differential conserted activity induced regulation of Nogo receptors (1-3), LOTUS and Nogo mRNA in mouse brain. PLoS One 8:e60892. CrossRef Medline

Kelly EA, Russo AS, Jackson CD, Lamantia CE, Majewska AK (2015) Proteolytic regulation of synaptic plasticity in the mouse primary visual cortex: analysis of matrix metalloproteinase 9 deficient mice. Front Cell Neurosci 9:369. CrossRef Medline

Lee H, Raiker SJ, Venkatesh K, Geary R, Robak LA, Zhang Y, Yeh HH, Shrager P, Giger RJ (2008) Synaptic function for the Nogo-66 receptor NgR1: regulation of dendritic spine morphology and activity-dependent synaptic strength. J Neurosci 28:2753–2765. CrossRef Medline

Lim ST, Chang A, Giuliano RE, Federoff HJ (2012) Ectodomain shedding of nectin-1 regulates the maintenance of dendritic spine density. J Neurochem 120:741–751. CrossRef Medline

McGee AW, Yang Y, Fischer QS, Daw NW, Strittmatter SM (2005) Experience-driven plasticity of visual cortex limited by myelin and Nogo receptor. Science 309:2222–2226. CrossRef Medline

Mironova YA, Giger RJ (2013) Where no synapses go: gatekeepers of circuit remodeling and synaptic strength. Trends Neurosci 36:363–373. CrossRef Medline

Monea S, Jordan BA, Srivastava S, DeSouza S, Ziff EB (2006) Membrane localization of membrane type 5 matrix metalloproteinase by AMPA receptor binding protein and cleavage of cadherins. J Neurosci 26:2300–2312. CrossRef Medline

Morrison CJ, Overall CM (2006) TIMP independence of matrix metalloproteinase (MMP)-2 activation by membrane type 2 (MT2)-MMP is determined by contributions of both the MT2-MMP catalytic and hemopexin C domains. J Biol Chem 281:26528–26539. CrossRef Medline

Nudo RJ, Wise BM, SiFuentes F, Milliken GW (1996) Neural substrates for the effects of rehabilitative training on motor recovery after ischemic infarct. Science 272:1791–1794. CrossRef Medline

Peixoto RT, Kunz PA, Kwon H, Mabb AM, Sabatini BL, Philpot BD, Ehlers MD (2012) Transsynaptic signaling by activity-dependent cleavage of neuroligin-1. Neuron 76:396–409. CrossRef Medline

Raiker SJ, Lee H, Baldwin KT, Duan Y, Shrager P, Giger RJ (2010) Oligodendrocyte-myelin glycoprotein and Nogo negatively regulate activity-dependent synaptic plasticity. J Neurosci 30:12432–12445. CrossRef Medline

Rodriguez A, Ehlenberger DB, Dickstein DL, Hof PR, Wearne SL (2008) Automated three-dimensional detection and shape classification of dendritic spines from fluorescence microscopy images. PLoS One 3:e1997. CrossRef Medline

Sanz R, Ferraro GB, Fournier AE (2015) IgLON cell adhesion molecules are shed from the cell surface of cortical neurons to promote neuronal growth. J Biol Chem 290:4330–4342. CrossRef Medline

Sanz RL, Ferraro GB, Girouard MP, Fournier AE (2017) Ectodomain shedding of limbic system-associated membrane protein (LSAMP) by ADAM metallopeptidases promotes neurite outgrowth in DRG neurons. Sci Rep 7:7961. CrossRef Medline

Suzuki K, Hayashi Y, Nakahara S, Kumazaki H, Prox J, Horiuchi K, Zeng M, Tanimura S, Nishiyama Y, Osawa S, Sehara-Fujisawa A, Saftig P, Yokoshima S, Fukuyama T, Matsuki N, Koyama R, Tomita T, Iwatsubo T (2012) Activity-dependent proteolytic cleavage of neuroligin-1. Neuron 76:410–422. CrossRef Medline

Takahashi H, Katayama K, Sohya K, Miyamoto H, Prasad T, Matsumoto Y, Ota M, Yasuda H, Tsumoto T, Aruga J, Craig AM (2012) Selective control of inhibitory synapse development by Slitrk3-PTPdelta trans-synaptic interaction. Nat Neurosci 15:389–398:S1–2. CrossRef Medline

Toth AB, Terauchi A, Zhang LY, Johnson-Venkatesh EM, Larsen DJ, Sutton MA, Umemori H (2013) Synapse maturation by activity-dependent

ectodomain shedding of SIRPalpha. Nat Neurosci 16:1417–1425. CrossRef Medline

Walmsley AR, McCombie G, Neumann U, Marcellin D, Hillenbrand R, Mir AK, Frentzel S (2004) Zinc metalloproteinase-mediated cleavage of the human Nogo-66 receptor. J Cell Sci 117:4591–4602. CrossRef Medline

Warren KM, Reeves TM, Phillips LL (2012) MT5-MMP, ADAM-10, and *N*-cadherin act in concert to facilitate synapse reorganization after traumatic brain injury. J Neurotrauma 29:1922–1940. CrossRef Medline

Wilczynski GM, Konopacki FA, Wilczek E, Lasiecka Z, Gorlewicz A, Michaluk P, Wawrzyniak M, Malinowska M, Okulski P, Kolodziej LR, Konopka W, Duniec K, Mioduszewska B, Nikolaev E, Walczak A, Owczarek D, Gorecki DC, Zuschratter W, Ottersen OP, Kaczmarek L (2008) Important role of matrix metalloproteinase 9 in epileptogenesis. J Cell Biol 180:1021–1035. CrossRef Medline

Wills ZP, Mandel-Brehm C, Mardinly AR, McCord AE, Giger RJ, Greenberg ME (2012) The nogo receptor family restricts synapse number in the developing hippocampus. Neuron 73:466–481. CrossRef Medline

Zemmar A, Weinmann O, Kellner Y, Yu X, Vicente R, Gullo M, Kasper H, Lussi K, Ristic Z, Luft AR, Rioult-Pedotti M, Zuo Y, Zagrebelsky M, Schwab ME (2014) Neutralization of Nogo-A enhances synaptic plasticity in the rodent motor cortex and improves motor learning *in vivo*. J Neurosci 34:8685–8698. CrossRef Medline